Article

A Compact Dual Gamma Neutron Detector Based on NaI(Tl+Li) Scintillator Readout with SiPM

Fengzhao Shen, Qibin Fu [ID], Tuchen Huang *[ID] and Wei Wang

Sino-French Institute of Nuclear Engineering and Technology, Sun Yat-sen University, Zhuhai 519082, China; shenfzh5@mail2.sysu.edu.cn (F.S.); fuqibin@mail.sysu.edu.cn (Q.F.); wangw223@mail.sysu.edu.cn (W.W.)
* Correspondence: huangtuchen@mail.sysu.edu.cn

Abstract: Sodium iodide crystal co-doped with thallium and lithium is a promising scintillator with wide application prospects for dual gamma neutron detection. In this study, a compact gamma/neutron detector was developed based on 2-inch NaI(Tl+Li) (NaIL) scintillator readout with 8×8 silicon photomultiplier (SiPM) array. Dedicated transimpedance amplifier circuit was developed for the SiPM array. The energy resolution and response linearity with the SiPM array were evaluated and compared to those obtained with photomultiplier tube (PMT) readout. The energy resolution for 661.6 keV gamma rays was measured as 7.0% and 6.5% with SiPM array and PMT, respectively. The linear response of the SiPM array is almost the same as that of the PMT in the energy range up to ~4 MeV. Neutron and gamma pulse shape discrimination was evaluated by acquiring the pulse waveforms with a digitizer (12 bit/250 MSPS) and off-line analysis. The best figure of merit (FOM) was measured as 3.75 for the SiPM array with optimized parameters, close to the performance measured with PMT (FOM = 4.07). The experimental results show that the NaIL scintillator readout with SiPM array exhibit energy resolution equivalent to NaI(Tl) gamma detectors and excellent neutron/gamma discrimination, making it especially suitable for compact devices requiring gamma and neutron dual detection capabilities.

Keywords: NaI(Tl+Li); SiPM; pulse shape discrimination; neutron detector; gamma detector

1. Introduction

Scintillators are widely used in radiation detection. In recent years, much interest exists for radiation detectors capable of measuring gamma rays and neutrons simultaneously due to increasing demands from security applications. Scintillators sensitive to both gamma and neutrons with pulse shape discrimination (PSD) ability have garnered significant interest [1–3]. Li-containing elpasolite single crystals such as CLYC and CLLB have been extensively studied because of their excellent neutron/gamma discrimination [4–7]. However, due to the complicated crystal growth process, these crystals are only commercially available in small sizes with high cost [8–10].

NaI(Tl) scintillator has been widely used for gamma detection with mature technology and low cost. It can be grown in ingots exceeding 100 L in volume. NaI(Tl) can be engineered to be thermal neutron sensitive by incorporating lithium into the crystal matrix [11]. The ^{6}Li co-doped NaI(Tl+Li) scintillator (abbreviated as NaIL in the text) exhibited excellent neutron/gamma discrimination and unchanged energy resolution [10,12], enabling broad application prospects in neutron detection, nuclear security, environmental monitoring, etc.

A photodetector is required to measure the luminescence of the scintillator. Photomultiplier tubes (PMTs) are the most commonly used photodetectors, but they are bulky and fragile, and are sensitive to magnetic fields. PMT also requires a high operating voltage ranging from hundreds of volts to thousands of volts. Silicon photomultiplier (SiPM), a semiconductor photodetector, has been widely used as an alternative to PMT for scintillator readout in recent years [13–16]. SiPM has the advantages of small volume and low operating voltage (tens of volts), especially suitable for compact devices [17,18]. Its insensitivity

to magnetic fields is also an excellent feature. However, SiPM also has disadvantages such as high dark noise, nonlinearity and gain variation with temperature [19]. In particular, since the size of a single SiPM is currently only up to 6 mm × 6 mm, SiPM array should be made for large crystals. The large capacitance and high noise of the SiPM array will affect the energy resolution and waveform discrimination, requiring special consideration and design on the front-end circuit.

A portable neutron gamma discrimination detector based on a 1-inch NaIL scintillator and SiPM array (4 × 4 array of 6 mm SiPM) was reported in Ref. [19]. The 16 SiPMs were directly connected in parallel, and the current was converted into voltage signal through a resistor. The pulse width of the output signal was greatly increased due to the huge capacitance of the SiPM array.

In this work, a compact dual gamma/neutron detector was developed based on a 2-inch NaIL scintillator readout with size-matched SiPM array. A dedicated front-end transimpedance amplifier circuit was developed for the SiPM array based on our previous research [15]. The waveforms, energy resolution and PSD performance of the NaIL scintillator readout with SiPM array were evaluated and compared to that measured with PMT.

2. Materials and Methods

2.1. Detector Design

The NaIL crystal used in the test was a Ø50.8 mm × 50.8 mm cylinder with 1% of enriched ^{6}Li doping. The crystal was polished on all surfaces and encapsulated in an aluminum cell with magnesium oxide (MgO) inside as reflector.

The NaIL crystal was coupled to an 8 × 8 ch SiPM array (ArrayJ-60035-64P, SensL, Cork, Ireland) with silicone oil, as shown in Figure 1. The J-series SiPMs are fabricated using through silicon via (TSV) technology to minimize dead space to only 0.2 mm between channels. Each SiPM in the array has an active area of 6.07 mm × 6.07 mm and consists of 22,292 avalanche photo diodes (APD) of 35 μm × 35 μm size. The photon detection efficiency (PDE) reaches maximum at 420 nm, well matched to the NaIL scintillator. Table 1 summarizes the main parameters of the SiPM array.


Figure 1. Assembly photos of NaIL scintillator readout with PMT (left) and SiPM array (right).

In order to reduce the influence of the large capacitance of the SiPM array on the pulse waveform, the SiPM array was divided into four groups for signal amplification (Figure 2). The SiPMs in each group were directly connected in parallel, followed by a transimpedance amplifier circuit (TIA) based on high-speed operational amplifier. The outputs of the four groups were finally summed to form a single output. The SiPMs were operated at 27.5 V bias voltage, corresponding to an overvoltage of 3 V.

Table 1. Main parameters of the SiPM array.

Manufacturer	SensL
Model	ArrayJ-60035-64P
Number of channels	64 (8 × 8 ch)
Active area/channel	6.07 mm × 6.07 mm
Number of APD cells/channel	22,292
Total number of APD cells	1,426,688
APD cell size	35 μm × 35 μm
Microcell fill factor	75%
Rated gain	2.9×10^6 (V_{OV} = 2.5V)
Spectral range	200–900 nm
Maximum sensitivity	420 nm
Photon detection efficiency (PDF)	38% (V_{OV} = 2.5V, λ = 420 nm)
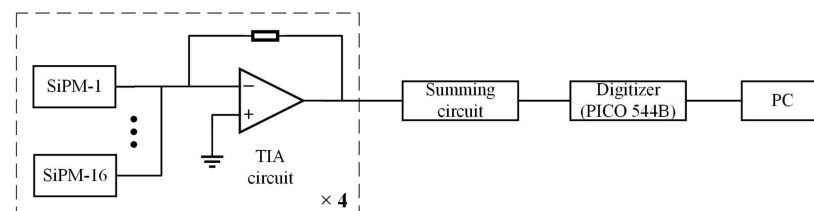
Figure 2. Schematic diagram of the amplifier circuit for SiPM array.

The NaIL scintillator was also tested with a 2-inch PMT (R6231-100, Hamamatsu, Shizuoka, Japan) for comparison (Figure 1). The PMT was operated at a high voltage of −1300 V. The anode of the PMT was connected to a TIA circuit similar to that used for the SiPM array. For both the PMT and SiPM array readout, the pulse waveforms were sampled by a digitizer (12 b/250 MSPS, Pico 5444B). The data were collected by the computer (PC) and analyzed offline using MATLAB software.

2.2. Experimental Setup

^{137}Cs, ^{60}Co, ^{22}Na, and ^{152}Eu gamma sources were used to test the energy resolution and linearity of the detector. The neutron and gamma discrimination were tested with an Am-Be neutron source as shown in Figure 3, resulting in a thermal neutron count rate of about 30 cps in the detector.

Figure 3. Experimental setup with Am-Be neutron source.

2.3. Emission Spectrometry

As shown in Figure 4, the emission spectrum of the crystal was measured by a monochromator spectrometer (OmniES-TUB-3007, Zolix, Beijing, China). A 50 kV monoblock X-ray source (TUB00082, Moxtek, Orem, UT, USA) was used to irradiate the crystal. Light from the crystal was diffracted by the grating system of the monochromator and collected by the PMT (R928, Hamamatsu, Shizuoka, Japan) working in single photon counting mode. The PMT signal was fed to a single photon counter (SPC) where single photoelectron pulses were registered. The SPC was synchronized with the monochromator using the software provided by the manufacturer.
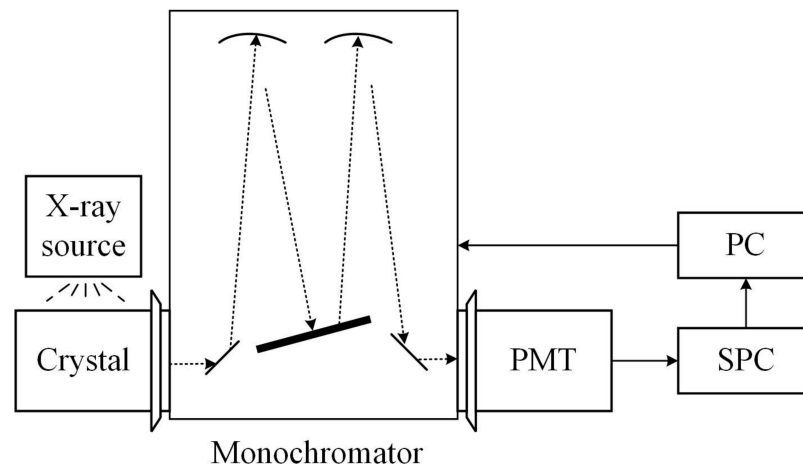

Figure 4. The diagram of experimental setup for emission spectrum measurement.

3. Results and Discussion

3.1. Emissions Spectra

The emission spectra of NaIL and NaI(Tl) scintillators excited by X-ray are shown in Figure 5. The main emission peak shifts slightly from 424 nm for NaI(Tl) to 429 nm for NaIL, which was caused by the change of crystal field and band-gap position due to the Li substitution [10].
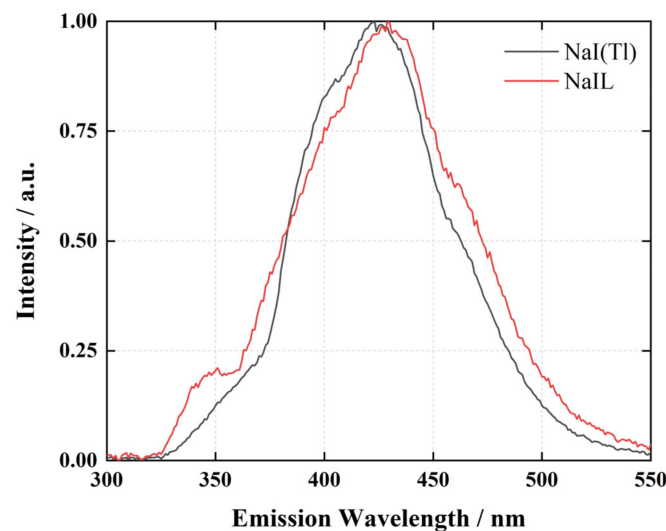

Figure 5. Emission spectra of NaIL and NaI(Tl) crystals excited by X-ray.

3.2. Energy Resolution and Linearity

The pulse amplitude spectrum was obtained by digital integration of the pulse waveforms with baseline correction. Figure 6 shows the spectra for ^{137}Cs gamma source measured with the NaIL crystal readout by PMT and SiPM array, using an integration window of 3 us. The energy resolutions for 661.6 keV gamma rays were measured as $6.5 \pm 0.2\%$ and $7.0 \pm 0.2\%$ FWHM (full width at half maximum) for the PMT and SiPM array, respectively. SiPM array shows slightly poorer energy resolution due to its high noise.
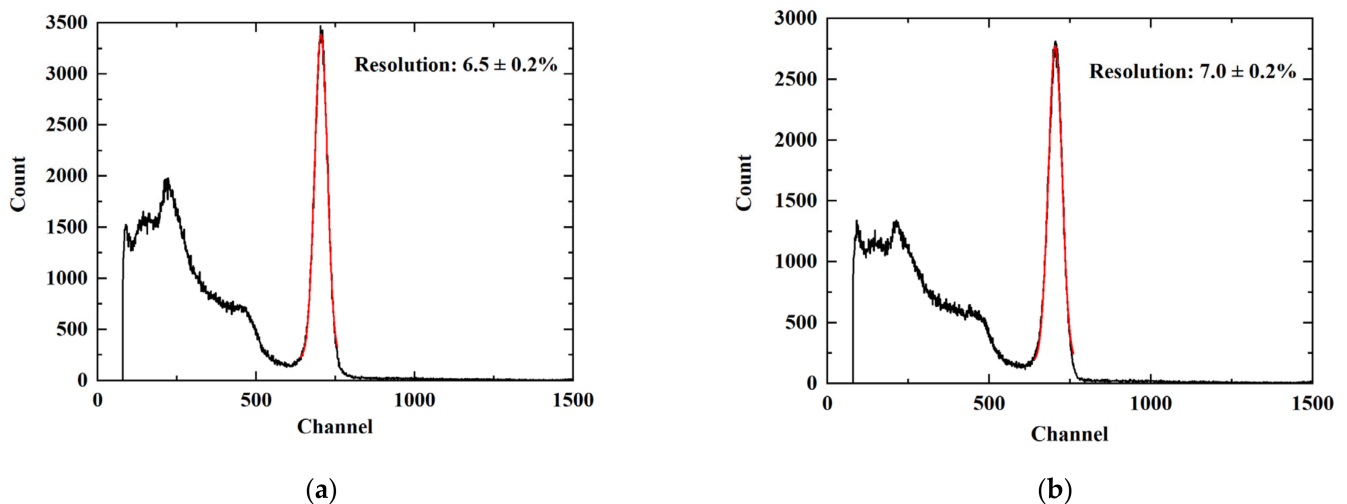

(**a**)　　　　　　　　　　　　　　　　　　　(**b**)

Figure 6. Pulse amplitude spectra of ^{137}Cs measured by NaIL readout with PMT (**a**) and SiPM array (**b**). The red curves show the Gaussian fitting results.

Linearity in energy measurement is a key metric for gamma spectroscopy. The nonlinearity of the measurement is the combined contribution of the nonlinearity of the crystal itself, the photodetector and the electronics. The nonlinearity of the transimpedance amplifier circuit can be ignored here. The nonlinearity of the PMT is a consequence of its structure as well as the voltage divider. For SiPM, when two or more photons hit a pixel at the same time, the output signal is the same due to its avalanche mode. The response linearity of SiPM depends on the total number of APD cells, the number of incident photons and dead time of APD cells in relation to the light pulse width [20].

Four spectra were measured with ^{22}Na (511, 1274.5 keV), ^{137}Cs (661.6 keV), ^{60}Co (1173, 1332.5 keV) and ^{152}Eu (121.8, 244.7, 344.3, 1085.8 and 1408 keV) gamma sources. The positions of the full energy peaks versus gamma-ray energies are shown in Figure 7. The solid line is a straight line drawn from the lowest two energy points (121.8 keV and 244.7 keV). The linearity performance measured with SiPM array is almost the same as that measured with PMT. The response of SiPM array shows a deviation of 2.8% at 1408 keV, compared to a deviation of 2.4% for PMT.
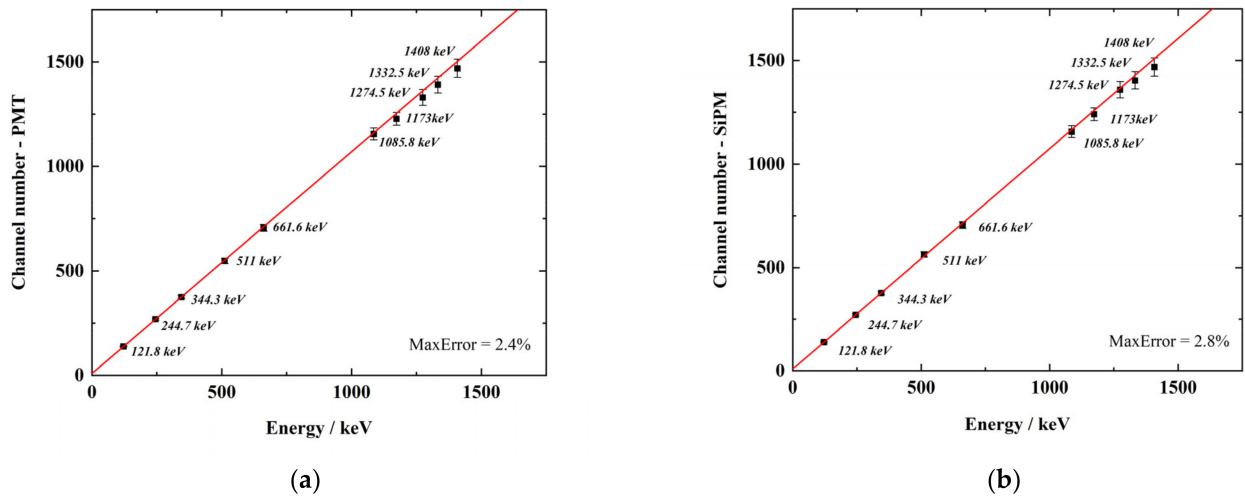
Figure 7. Linearity of the NaIL crystal readout with PMT (**a**) and SiPM array (**b**).

3.3. Waveforms

Adding lithium to the NaI(Tl) will increase the duration of the luminescence pulse. The lengthening of the pulse is caused by the additional electron traps created by the lithium atoms distorting the crystal lattice. The traps are shallow enough to eventually release their electrons, resulting in an increase in the pulse length [10].

Figure 8 shows the representative gamma and neutron signal waveforms. These waveforms are the average shapes of 100 signals and are normalized for comparison. As shown in Figure 8a, the pulse length of the gamma waveform increased slightly for the NaIL compared to standard NaI(Tl). Neutron pulses decay faster than gamma pulses for NaIL, which enables pulse shape discrimination. For SiPM readout, due to the large capacitance of the SiPM array, the waveforms exhibit a slower response compared to those measured by PMT.
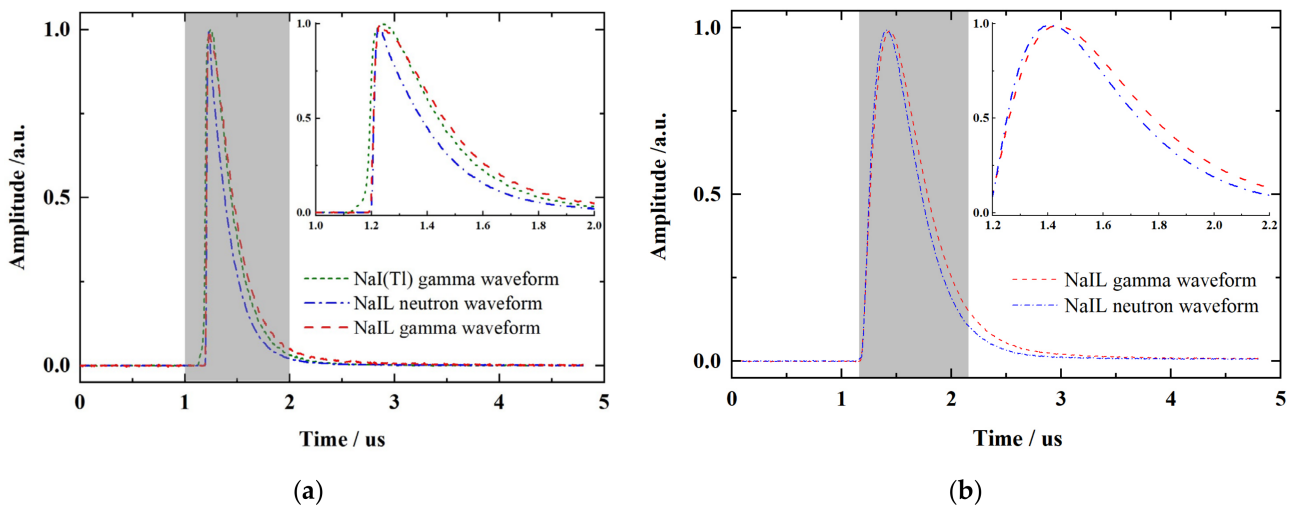

Figure 8. Average gamma and neutron waveforms measured with PMT (**a**) and SiPM array (**b**).

3.4. Pulse Shape Discrimination

The pulse shape discrimination was implemented by comparing the charges integrated within two windows of different lengths [15]. The PSD value can be calculated as:

$$\text{PSD} = \frac{Q_L - Q_S}{Q_L} \tag{1}$$

where Q_S and Q_L are the integrations within the short and long windows, respectively, with baseline correction. The baseline was calculated as the average value of the samples within the time window from 900 ns before trigger to 100 ns before trigger. The short and long windows were optimized to [300 ns, 1600 ns] and [700 ns, 2000 ns] for PMT and SiPM array, respectively.

Figure 9 shows the 2D histograms of PSD value versus energy measured with the Am-Be neutron source. The energy was calibrated with the ^{137}Cs source. Neutrons exhibit lower PSD values, clearly distinguished from gamma rays. The gamma equivalent energy of thermal neutron was calculated from the center position obtained by a Gaussian fit of the thermal neutron peak, which were measured as 3.79 ± 0.07 MeVee for PMT and 3.77 ± 0.06 MeVee for SiPM array. This result also shows that the linear response of the SiPM array is almost the same as that of the PMT even at energy higher than 3 MeV.
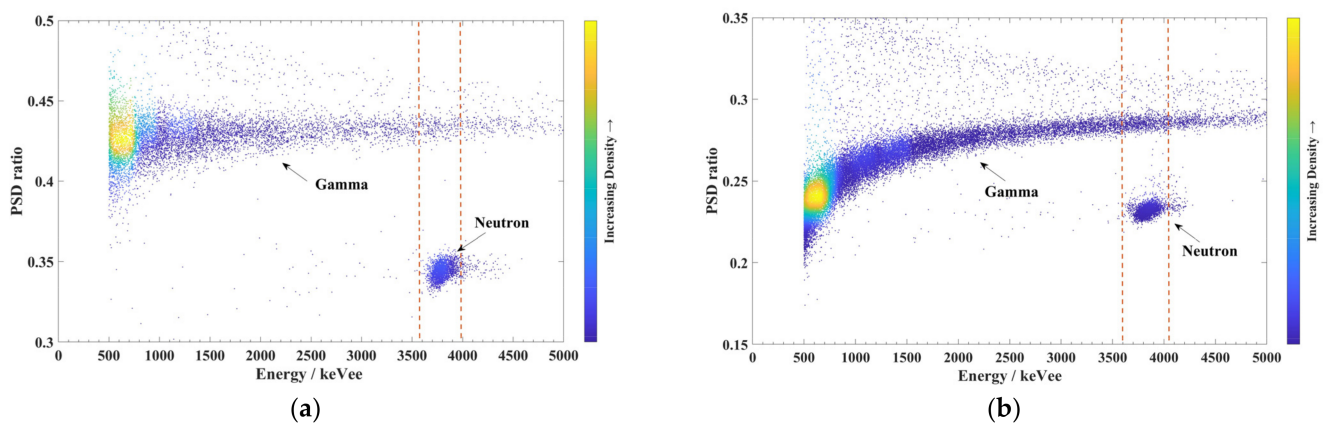

Figure 9. The PSD histograms of the NaIL readout with PMT (**a**) and SiPM array (**b**).

The distortion in the low-energy region of the PSD histogram measured with SiPM array was due to the increase of the rise time of the signal pulse (~250 ns for SiPM array compared to ~40 ns for PMT). When the signal amplitude is relatively small, a longer rise time will result in larger fluctuations in the trigger position.

Figure 10 shows the 1D distributions of event counts versus the PSD values with selected data in the energy window for $\pm 3\sigma$ around the center of the neutron distribution (as indicated by the dashed lines in Figure 9). The figure of merit (FOM) is calculated as [15]:

$$\text{FOM} = \frac{|P_1 - P_2|}{W_1 + W_2} \qquad (2)$$

where P and W are the centroids and FWHM values of the two peaks in the PSD distribution, obtained by fitting the two peaks with Gaussian function as shown by the red curves in Figure 10. The FOM was measured as 4.07 ± 0.17 and 3.75 ± 0.07 for the PMT and SiPM array, respectively. Due to the large capacitance and high noise of the SiPM array, the FOM is slightly lower than that measured with PMT, but still shows excellent discrimination performance.
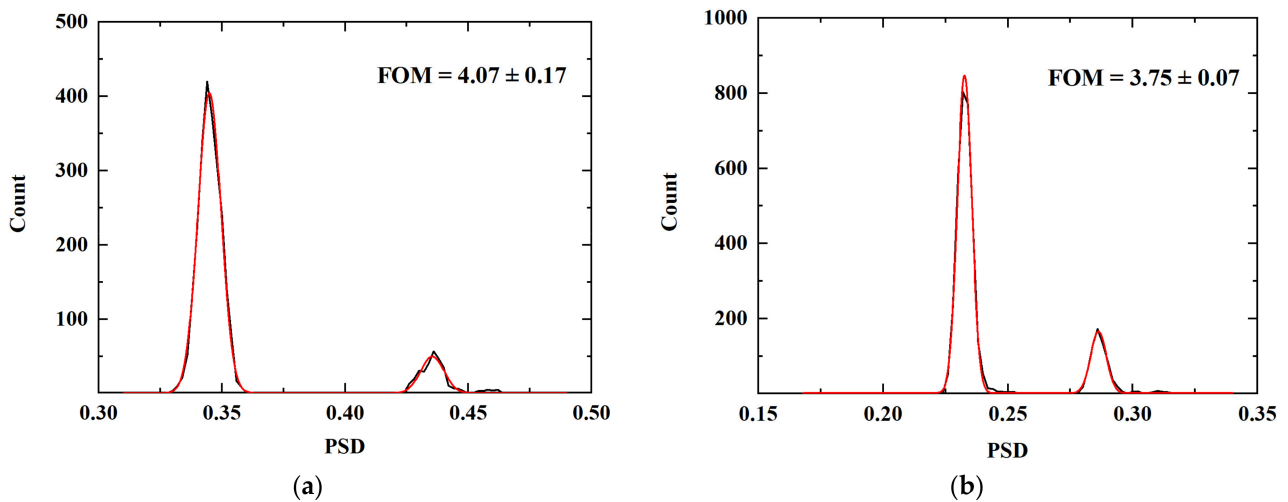
Figure 10. The 1D distributions of event counts versus the PSD values for PMT (**a**) and SiPM array (**b**). The red curves show the Gaussian fitting results.

4. Conclusions

A compact dual gamma/neutron detector was developed based on a 2-inch NaIL scintillator readout with SiPM array. Its performances were evaluated and compared to those obtained with PMT readout. The emission spectrum and the pulse waveforms of gamma and neutron signals were measured. The energy resolution for 661.6 keV gamma rays was measured as 7.0% with SiPM array, slightly worse than the value of 6.5% measured with PMT. The linear response of the SiPM array is almost the same as that of the PMT in the energy range up to ~4 MeV. For pulse shape discrimination, an FOM of 3.75 was obtained with SiPM array, close to the performance measured with PMT (FOM = 4.07). The experimental results show that the NaIL scintillator readout with SiPM array exhibit energy resolution equivalent to common NaI(Tl) gamma detectors and excellent neutron/gamma discrimination, making it especially suitable for compact devices requiring both gamma and neutron detection capabilities.

Author Contributions: Conceptualization, W.W. and Q.F.; methodology, F.S. and T.H.; software, F.S.; validation, T.H. and Q.F.; investigation, Q.F.; data curation, F.S.; writing—original draft preparation, F.S.; writing—review and editing, T.H. and Q.F.; funding acquisition, T.H. All authors have read and agreed to the published version of the manuscript.

Institutional Review Board Statement: Not applicable.

Informed Consent Statement: Not applicable.

Data Availability Statement: Not applicable.

Conflicts of Interest: The authors declare no conflict of interest.

References

1. Lee, C.; Yoon, S.; Won, B.; Seo, H.; Park, S.; Ahn, S. Comparative study of dual neutron/gamma scintillation detectors. *J. Radioanal. Nucl. Chem.* **2021**, *330*, 555–561. [CrossRef]
2. Pérez-Loureiro, D.; Kamaev, O.; Bentoumi, G.; Li, L.; Jewett, C.; Thompson, M. Evaluation of CLYC-6 and CLYC-7 scintillators for detection of nuclear materials. *Nucl. Instrum. Methods Phys. Res. Sect. A* **2021**, *1012*, 165622. [CrossRef]
3. Glodo, J.; Hawrami, R.; Shah, K.S. Development of Cs_2LiYCl_6 scintillator. *J. Cryst. Growth* **2013**, *379*, 73–78. [CrossRef]
4. Glodo, J.; van Loef, E.; Hawrami, R.; Higgins, W.M.; Churilov, A.; Shirwadkar, U.; Shah, K.S. Selected Properties of Cs_2LiYCl_6, $Cs_2LiLaCl_6$, and $Cs_2LiLaBr_6$ Scintillators. *IEEE Trans. Nucl. Sci.* **2011**, *58*, 333–338. [CrossRef]
5. McDonald, B.S.; Myjak, M.J.; Zalavadia, M.A.; Smart, J.E.; Willett, J.A.; Landgren, P.C.; Greulich, C.R. A wearable sensor based on CLYC scintillators. *Nucl. Instrum. Methods Phys. Res. Sect. A* **2016**, *821*, 73–80. [CrossRef]

6. Glodo, J.; Hawrami, R.; van Loef, E.; Shirwadkar, U.; Shah, K.S. Pulse Shape Discrimination with Selected Elpasolite Crystals. *IEEE Trans. Nucl. Sci.* **2012**, *59*, 2328–2333. [CrossRef]
7. Yang, K.; Menge, P.R. Pulse shape discrimination of Cs_2LiYCl_6:Ce^{3+} scintillator from -30 °C to 180 °C. *Nucl. Instrum. Methods Phys. Res. Sect. A* **2015**, *784*, 74–79. [CrossRef]
8. Caifeng, L.; Jianguo, Q.; Jun, X.; Tonghua, Z.; Xinxin, L.; Li, A.; Yunfeng, M.; Pu, Z.; Junjie, S.; Li, J.; et al. Particle discrimination and fast neutron response for a NaIL:Tl and a NaI:Tl scintillator detector. *Nucl. Instrum. Methods Phys. Res. Sect. A* **2020**, *978*, 164372. [CrossRef]
9. Liang, F.; Brands, H.; Hoy, L.; Preston, J.; Smith, J. Lithium-Loaded Scintillators Coupled to a Custom-Designed Silicon Photomultiplier Array for Neutron and Gamma-Ray Detection. *IEEE Trans. Nucl. Sci.* **2018**, *65*, 2162–2168. [CrossRef]
10. Yang, K.; Menge, P.R.; Ouspenski, V. Li co-doped NaI:Tl (NaIL)—A Large Volume Neutron-Gamma Scintillator with Exceptional Pulse Shape Discrimination. *IEEE Trans. Nucl. Sci.* **2017**, *64*, 2406–2413. [CrossRef]
11. Sangster, J.; Pelton, A.D. Phase Diagrams and Thermodynamic Properties of the 70 Binary Alkali Halide Systems Having Common Ions. *J. Phys. Chem. Ref. Data* **1987**, *16*, 509–561. [CrossRef]
12. Tao, M.; Wang, Z.; Chen, Q.; Li, F.; Qi, J.; Qi, P.; Gao, T.; Zhao, Q.; Zhang, Z.; Zhu, B.; et al. Design and performance of a NaIL detector for neutron/gamma discrimination. *J. Instrum.* **2021**, *16*, P08067. [CrossRef]
13. Huang, T.; Fu, Q.; Lin, S.; Wang, B. NaI(Tl) scintillator read out with SiPM array for gamma spectrometer. *Nucl. Instrum. Methods Phys. Res. Sect. A* **2017**, *851*, 118–124. [CrossRef]
14. Huang, T.; Fu, Q.; Yuan, C.; Lin, S. A gamma and neutron phoswich read out with SiPM for SPRD. *Nucl. Instrum. Methods Phys. Res. Sect. A* **2018**, *881*, 48–52. [CrossRef]
15. Huang, T.; Zhang, Z. Characterization of 1-inch CLYC scintillator coupled with 8×8 SiPM array. *Nucl. Instrum. Methods Phys. Res. Sect. A* **2021**, *999*, 165225. [CrossRef]
16. Shen, F.; Pan, Y.; Fu, Q.; Lin, S.; Huang, T.; Wang, W. PSD performance of EJ-276 and EJ-301 scintillator readout with SiPM array. *Nucl. Instrum. Methods Phys. Res. Sect. A* **2022**, *1039*, 167148. [CrossRef]
17. Del Guerra, A.; Belcari, N.; Giuseppina Bisogni, M.; LLosa, G.; Marcatili, S.; Ambrosi, G.; Corsi, F.; Marzocca, C.; Dalla Betta, G.; Piemonte, C. Advantages and pitfalls of the silicon photomultiplier (SiPM) as photodetector for the next generation of PET scanners. *Nucl. Instrum. Methods Phys. Res. Sect. A* **2010**, *617*, 223–226. [CrossRef]
18. Carnesecchi, F.; Agrawal, N.; Alici, A.; Antonioli, P.; Arcelli, S.; Basile, M.; Bellini, F.; Cavazza, D.; Cifarelli, L.; Cindolo, F.; et al. Experimental study of the time resolution of SiPM coupled to scintillator. *Nucl. Instrum. Methods Phys. Res. Sect. A* **2020**, *982*, 164484. [CrossRef]
19. Zhang, Z.; Wang, D.; Feng, S.; Ye, Z.; Zhou, T.; Zheng, Z.; Wang, F.; Zhao, C.; Wang, Z.; Bai, L.; et al. A portable neutron gamma discrimination detector based on NaIL and SiPM. *J. Instrum.* **2022**, *17*, T06005. [CrossRef]
20. Grodzicka, M.; Moszynski, M.; Szczesniak, T.; Szawlowski, M.; Baszak, J. Characterization of 4×4 ch MPPC array in scintillation spectrometry. *J. Instrum.* **2013**, *8*, P09020. [CrossRef]